ELSEVIER

www.elsevier.nl/locate/jorganchem

Journal of Organometallic Chemistry 606 (2000) 112–124

Journal of Organometallic Chemistry

Pyridinylimine-based nickel(II) and palladium(II) complexes: preparation, structural characterization and use as alkene polymerization catalysts

Timo V. Laine *, Ulla Piironen, Kristian Lappalainen, Martti Klinga, Erkki Aitola, Markku Leskelä

Laboratory of Inorganic Chemistry, Department of Chemistry, PO Box 55, FIN-00014 University of Helsinki, Finland

Received 1 September 1999; received in revised form 3 April 2000

Abstract

Preparation of four dimeric nickel(II) complexes and three monomeric palladium(II) complexes bearing didentate pyridinylimine ligands is described. The solid-state structures of these compounds have been determined by single-crystal X-ray diffraction. After activation with methylaluminoxane (MAO) the nickel compounds were used as catalysts in ethylene polymerization producing nearly linear or primarily methyl-branched polymers. The effect of ligand environment was most evident on degree of branching, while catalytic activity and molecular weight of the polymer were more dependent on the general catalyst composition as well as reaction conditions. Activation of the dichloropalladium(II) complexes with MAO yields highly active catalysts for the polymerization of bicyclo[2.2.1]hept-2-ene (norbornene) whereas only low conversions ($< 20\%$) were achieved with cationic compounds obtained from two of the neutral palladium complexes by reaction with $AgBF_4$.

Keywords: Nickel; Palladium; Nitrogen ligand; Crystal structures; Polymerization; Catalysis; Ethylene; Norbornene

1. Introduction

During the past two decades transition-metal-based catalytic applications in alkene polymerization have rapidly evolved from the realms of academic laboratories into full-scale industrial processes [1]. Consequently various highly active catalyst systems, which contain well-defined active centers and catalyst structures thus enabling the control of polymer properties by fine-tuning of the catalyst precursor itself [2], have been discovered. Some of these new catalysts, particularly Group 4 metallocenes [3–6], are already utilized by the plastics industry [2].

Although the group of catalytically applicable metals is expanding beyond the early transition metals [7], as exemplified by the recently reported homogeneous chromium [8], iron, and cobalt systems [9,10], late transition metal compounds have traditionally been considered as poor polymerization catalysts for simple alkenes [11], such as ethylene and propylene, leading to short-chain products due to the highly competitive chain termination step [12,13]. In 1995 the group of Brookhart, however, was able to produce high molecular weight polyethylene with nickel- and palladium-based catalysts [14,15]. The key discovery here was the use of sterically demanding 1,4-diazabutadiene ligands, which effectively block the axial coordination sites thus impeding chain termination [14,16,17]. When the bulkiness of the aryl groups attached to the imino nitrogens is reduced, the product composition can be shifted towards linear oligomers [18,19].

Late transition metals can also be used in the polymerization of the strained cycloalkene bicyclo[2.2.1]hept-2-ene (norbornene) by addition-type vinylic polymerization yielding a saturated polymer, poly(2,3-bicyclo[2.2.1]heptene), which contains intact bicyclic units [20–22]. Catalyst systems for this reaction

* Corresponding author. Present address: Borealis Polymers Oy, PO Box 330, FIN-06101 Porvoo, Finland. Tel.: +358-9-19140223; fax: +358-9-19140198.

E-mail address: timo.laine@borealisgroup.com (T.V. Laine).

0022-328X/00/$ - see front matter
PII: S0022-328X(00)00291-6

are typically based on Group 4 and 10 metals, especially titanium(IV), zirconium(IV), and palladium(II). Also some chromium(III) [23] and cobalt(II) [24] compounds have been reported to promote vinylic polymerization.

Earliest palladium-containing norbornene polymerization catalysts consisted of simple palladium(II) salts or their nitrile and phosphine adducts [25,26]. These compounds usually required long polymerization times and resulted in only low to moderate yields. The development of cationic catalyst species in which the Pd^{2+} center is surrounded by four neutral, weakly coordinating alkylnitrile ligands [27] established the basis for the present catalyst generation of sharply increased activity [20–22,28–31]. In other currently investigated catalytic systems also allyl [29,32–34], alkyl [33,35] or diamine [36] ligands are incorporated. Activation of various palladium-based precursors can be achieved using methylaluminoxane (MAO) as well producing efficient catalysts for this reaction [35,37].

Recently we have reported the preparation [38] of novel nickel-based ethylene polymerization catalysts [39] bearing an unsymmetrical didentate pyridinylimine ligand which combines specific features from the bipyridine-type alkene oligomerization catalyst [18] and the sterically hindered α-diimine-based polymerization system [14]. Similar systems have also appeared in recent patent applications [40–42]. In order to study the effects of different ligand substitution patterns on the polymerization behavior of these compounds four new nickel(II) complexes (**6**–**9**), which contain substituted 2-pyridinylimine ligands (**2**–**5**), have been synthesized and used as catalysts in ethylene polymerization after activation with methylaluminoxane (Scheme 1). By extending the same basic ligand structure to palladium(II) compounds we have prepared three dichloropalladium complexes (**10**–**12**) bearing ligands **1**–**3** and investigated the catalytic behavior of both cationic (**13**, **14**) and MAO-activated complexes in norbornene polymerization. The palladium compounds could not be activated with MAO for ethylene polymerization [39], even though some ethylene and propylene oligomerization activity has been reported using an ion-pair activated palladium complex of ligand **4** [43].

2. Results and discussion

2.1. Synthesis of catalyst precursors

Since pyridine-based aromatic aldehydes readily react with substituted phenylamines, including sterically hindered 2,6-dialkyl derivatives, to form pyridinylimines [44], ligands **1**–**3** could be prepared by simple one-step condensation of 2-pyridinecarboxaldehydes with the appropriate phenylamines. The synthesis of analogous compounds starting from aromatic ketones, however, is usually less successful [45] requiring more severe reaction conditions and prolonged reaction times. In the case of ligands **4** and **5** moderate yields (33–34%) were achieved when a few drops of concentrated H_2SO_4 was introduced as catalyst and Na_2SO_4 was used to remove the water formed during the reaction. This method is a modified version of the literature procedure for bulky benzophenone *N*-arylimines, in which tetraethyl orthosilicate is utilized to eliminate water from the reaction mixture [46]. All attempts to improve yields by varying the acid catalyst used or the ketone–amine ratio failed.

Subsequent complex formation was accomplished by treatment of dibromo(1,2-dimethoxyethane)nickel(II) or (1,5-cyclooctadiene)palladium(II)chloride with a slight excess of the corresponding ligand affording compounds **6**–**12** in good yields (55–77%). In all cases complex formation started within 1 h, which could be observed when the precipitation of the product commenced, but stirring was continued overnight to maximize product yields. However, conversion of the neutral dichloropalladium(II) complexes **10**–**12** into the

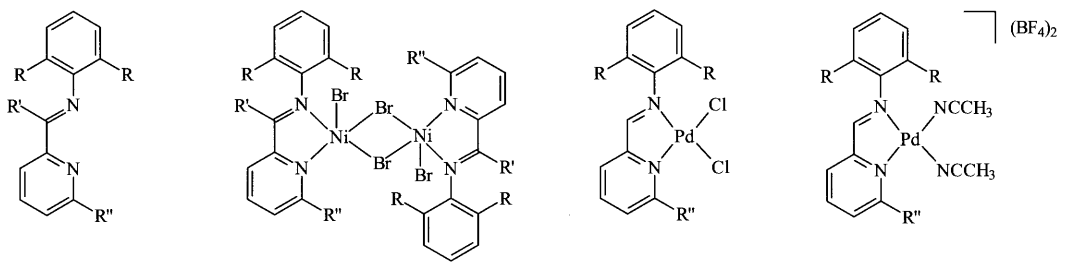

1: R = *i*Pr; R' = R'' = H
2: R = Me; R' = R'' = H
3: R = *i*Pr; R' = H; R'' = Me
4: R = *i*Pr; R' = Me; R'' = H
5: R = *i*Pr; R' = Ph; R'' = H

6: R = Me; R' = R'' = H
7: R = *i*Pr; R' = H; R'' = Me
8: R = *i*Pr; R' = Me; R'' = H
9: R = *i*Pr; R' = Ph; R'' = H

10: R = *i*Pr; R'' = H
11: R = Me; R'' = H
12: R = *i*Pr; R'' = Me

13: R = *i*Pr; R'' = H
14: R = *i*Pr; R'' = Me

Scheme 1.

cationic species using silver tetrafluoroborate proved to be somewhat difficult. Long reaction times of up to 3 days were needed in order to reach reasonable yields, but in the case of the dimethylphenylamine complex **11** this led to decomposition and, therefore, the corresponding ion-pair compound could not be obtained.

For pyridinylimines such as compounds **1**–**4**, which either are lacking the bridge substituent or contain a small side group attached to the imino carbon, unambiguous peak assignment of the ^{1}H-NMR spectra can be made [38,47], but for the phenyl substituted ligand **5** the interpretation of signals fails in the aromatic region of the spectrum. Therefore, the bulky nature of the associated phenyl group seems to play an important role. While the less substituted aromatic imines have a strong preference towards the *E*-conformation for steric reasons [45], in the case of compound **5** the formation of both isomers should be as favorable, since the two α-substituents are now nearly equal in steric bulk and the geometric preference can not be distinguished any longer, thus, giving rise to a mixture of *E*- and *Z*-isomers, as has been observed with analogous benzophenone-derived *N*-aryl imines [45].

^{1}H-NMR spectroscopic analysis of the ligands and the palladium complexes reveals some changes in chemical shifts. Separation of the isopropyl methyl peaks, as in this case of compound **10** [38], is also observed for complexes **12**–**14** whereas in compound **11**, which contains the smaller methyl groups in the 2- and 6-positions of the phenyl ring, only one peak for the methyl groups is detected. On the pyridine side of the complex the effect of the neighboring chloride is well displayed. When a chlorine atom is attached to palladium the chemical shift of the proton (or in complex **12**, the protons of the methyl group) in the 6-position of the pyridine ring is transferred downfield by 0.44–0.51 ppm. This interaction between the pyridine methyl group and the chloro ligand in complex **12** can be seen also in the solid state structure (for further structural analysis, see chapter 2.2). After replacement of the chlorides with acetonitrile molecules in the cationic complexes **13** and **14**, the values for the chemical shifts of the *ortho* substituent protons return to the proximity of the values observed for free ligands. Yet another consequence of complex formation can be seen when signals from the pyridine ring are analyzed. In the free ligands the signal of the hydrogen in the 3-position is shifted to lower field, but this interaction disappears after incorporation of metal and the usual order of signals originating from the pyridine *meta* and *para* protons [38,47] is restored. Due to interference by the associated metal NMR spectroscopic measurements could not be performed for the nickel complexes **6**–**9**.

2.2. Solid state structures

Crystallization from dichloromethane (for **9**), acetone (for **12**) or a mixture of acetone and pentane (1:1 for **6** and **11**, 2:1 for **7**, and 3:1 for **8**) yielded deep orange or orange–yellow crystals suitable for crystal structure determinations. The crystal data, together with the data collection and structure refinement parameters are presented in Table 1. Selected bond lengths and angles for the nickel compounds **6**–**9** are given in Table 2. Selected bond lengths and angles for the palladium complexes are given in Table 3; the previously reported related values of complex **10** are included for comparison. In each compound the solid-state structures are stabilized only by van der Waals forces between the molecules.

All nickel complexes crystallize as centrosymmetric dimers with two ligand nitrogen atoms (N1 and N8), one terminal bromine (Br2) and two bridging bromine atoms (Br1 and Br1a) forming the coordination sphere around each five-coordinate nickel center. The asymmetric unit of **7**, however, contains the halves of two independent, nearly identical molecules (Fig. 2) whereas a half of only one complex molecule can be found in the asymmetric unit of compounds **6**, **8**, and **9** (see Fig. 1Figs. 3 and 4, respectively).

The coordination polyhedra can be regarded as slightly deformed trigonal bipyramids in which the equatorial plane includes the nitrogen of the imino bridge in the ligand (N8), the terminal bromine (Br2) and one of the two μ-Br atoms (Br1a in **7**, Br1 in **6**, **8**, and **9**) while the nickel center is slightly deviated from the triangular plane (values ranging from 0.0371(11) Å in **7** to 0.171(2) Å in **8**). The pyridine nitrogen (N1) and the other constituent of the bromine bridge (Br1 in **7**, Br1a in **6**, **8**, and **9**) occupy the axial coordination sites. Complex **9** has the bipyramidal structure most distorted towards a square-based pyramid with the most acute angle (166.67(11)°) in the vertical axis (N1–Ni–Br1a) and one of the equatorial angles being extended to 145.74(10)°. Nevertheless, in all cases the vertical axis of the bipyramid is tilted from the position perpendicular to the equatorial plane due to the narrow nitrogen–nickel–nitrogen angle (79.4(2)° in **6**, 80.29(13) and 80.55(13)° in **7**, 79.61(19)° in **8**, and 79.06(14)° in **9**) resulting from the relatively small bite size of the ligand.

Structural parameters in all four nickel complexes of this study followed the trends found previously for the analogous dibromonickel(II) compound bearing 2,6-bis(1-methylethyl)-*N*-(2-pyridinylmethylene)phenylamine as the ligand [38]. All the relevant bond lengths were in accord with the earlier report with the exception that for compounds **6** and **7** the bond to the pyridine nitrogen (N1) is the shorter of the two nickel–nitrogen bonds connecting the metal center and

Table 1
Crystallographic data for complexes **6**–**9**, **11**, and **12**

	6	**7**	**8**	**9**	**11**	**12**
Empirical formula	$C_{28}H_{28}Br_4N_4Ni_2$	$C_{38}H_{48}Br_4N_4Ni_2$	$C_{38}H_{48}Br_4N_4Ni_2$	$C_{48}H_{52}Br_4N_4Ni_2{\cdot}4CH_2Cl_2$	$C_{14}H_{14}Cl_2N_2Pd$	$C_{19}H_{24}Cl_2N_2Pd$
Formula weight	857.55	997.82	997.82	1461.69	387.60	457.73
Crystal color and form	Orange, prismatic	Red, prismatic	Red, prismatic	Red, prismatic	Yellow, prismatic	Orange, prismatic
Crystal system	Monoclinic	Monoclinic	Monoclinic	Monoclinic	Triclinic	Orthorhombic
Space group	$P2_1/n$ (no. 14)	$P2_1/c$ (no. 14)	$P2_1/n$ (no. 14)	$P2_1/c$ (no. 14)	$P\bar{1}$ (no. 2)	$P2_12_12_1$ (no. 19)
a (Å)	12.118(7)	10.319(4)	14.311(4)	11.971(4)	11.813(4)	12.496(6)
b (Å)	10.425(3)	19.802(4)	10.240(4)	14.369(3)	13.017(5)	16.137(6)
c (Å)	12.438(7)	20.691(6)	14.335(5)	18.180(4)	9.761(4)	9.996(7)
α (°)	90	90	90	90	96.67(3)	90
β (°)	102.75(4)	93.84(3)	110.95(2)	107.04(2)	97.89(3)	90
γ (°)	90	90	90	90	93.66(3)	90
V (Å^3)	1532.5(13)	4218(2)	1961.8(12)	2989.9(13)	1471.8(10)	2015.7(19)
Z	2	4	2	2	4	4
D_{calc} (g cm^{-3})	1.858	1.571	1.689	1.624	1.749	1.508
Absorption coefficient μ (mm^{-1})	6.467	4.711	5.065	3.698	1.610	1.188
F(000)	840	2000	1000	1464	768	928
Crystal size (mm)	$0.23\times0.11\times0.10$	$0.48\times0.40\times0.35$	$0.30\times0.25\times0.22$	$0.30\times0.26\times0.24$	$0.25\times0.20\times0.15$	$0.50\times0.20\times0.10$
Scan mode	ω–2θ	ω–2θ	ω–2θ	ω–2θ	ω–2θ	ω–2θ
θ_{max} (°)	26.49	25.00	25.01	25.00	25.00	26.47
Number of unique reflections	2569	6833	3101	4784	4933	2295
Number of observed reflections [$I>2\sigma(I)$]	2011	5625	2512	3952	4442	2163
Number of parameters	172	433	222	316	343	247
Goodness-of-fit on F^2 [a]	1.030	1.033	1.027	1.021	1.033	1.045
Final R indices [$I>2\sigma(I)$] [b]	$R=0.0485$, $wR=0.0909$	$R=0.0387$, $wR=0.0793$	$R=0.0479$, $wR=0.1060$	$R=0.0441$, $wR=0.0981$	$R=0.0355$, $wR=0.0908$	$R=0.0439$, $wR=0.1079$
R indices (all data) [b]	$R=0.0713$, $wR=0.0980$	$R=0.0546$, $wR=0.0839$	$R=0.0656$, $wR=0.1130$	$R=0.0585$, $wR=0.1031$	$R=0.0409$, $wR=0.0936$	$R=0.0471$, $wR=0.1097$
Largest differential peak and hole (e Å^{-3})	0.526 and −0.664	0.440 and −0.386	0.625 and −0.572	0.591 and −1.127 [c]	0.469 and −0.816	1.345 [d] and −1.265 [e]

[a] $S=\{\Sigma[w(F_o^2-F_c^2)^2]/(n-p)\}^{0.5}$ where n = data and p = parameters.
[b] $R=\Sigma||F_o|-|F_c||/\Sigma|F_o|$ with $F>4\Sigma(F)$; function minimized is $wR=\{\Sigma[w(F_o^2-F_c^2)^2]/\Sigma[w(F_o^2)^2]\}^{0.5}$.
[c] Minimum residual electron density −1.127 e Å^{-3}; hole coordinates $x=0.4818$, $y=0.9406$, z = 0.1179; distance to nearest atom (Br1) 0.92 Å.
[d] Maximum residual electron density 1.345 e Å^{-3}; peak coordinates $x=0.0581$, $y=0.1540$, z = 0.4013; distance to nearest atom (Pd) 0.99 Å.
[e] Minimum residual electron density −1.265 e Å^{-3}; hole coordinates $x=0.0233$, $y=0.1580$, z = 0.4781; distance to nearest atom (Pd) 0.95 Å.

the ligand. Also the intramolecular nickel–nickel distances (between 3.656(2) Å in **6** and 3.7158(17) Å in **8**) are well corresponding with the value (3.658 Å) obtained previously for the analogous complex [38]. Furthermore, similar behavior of the aryl ring attached to the imino nitrogen of the ligand was observed with the angles between the pyridine ring and the phenyl group of the imino side arm varying from 83.99(16)° in the first molecule of complex **7** to 87.0(2)° in complex **6**. Even the phenyl substituent in complex **9** was found to adopt a position close to perpendicular (72.9(2)°) to the C=N bond, as has been postulated in the literature [45].

Both palladium compounds, in turn, crystallize as discrete monomers with the expected square-planar coordination sphere around the palladium center consisting of two chlorine atoms (Cl1 and Cl2) and two nitrogen atoms of the ligand (N1 and N8). The asymmetric unit of **11**, however, contains two independent, closely resembling molecules (see Fig. 5) whereas only one molecule is found in the asymmetric unit of complex **12** (see Fig. 6).

In both cases the square structure is again slightly deformed as a result of the narrow nitrogen–palladium–nitrogen angle (80.19(15) and 80.38(15)° in **11**, 80.8(2)° in **12**) as in related pyridinylimine [38,47] and bipyridine [48–50] complexes. The methyl group in the pyridine 6-position of compound **12** generates even greater distortion with the neighboring chlorine atom (Cl1) protruding as much as 0.459(7) Å away from the ligand coordination plane, which can be defined as the plane of the five-membered metallacycle Pd–N1–C6–C7–N8. In the same process the palladium–pyridine bond (Pd–N1) is extended (2.114(5) Å) compared to the bonding distances (2.025(4)–2.028(3) Å) of complexes

10 and **12** (see Table 3), corresponding to the slanting of the palladium coordination sphere towards the side of the phenyl ring. The other chloride (Cl2) twists only slightly, 0.143(7) Å, to the same side as Cl1. Similar behavior has been reported also for a palladium complex bearing the unsymmetric 6-methyl-2,2′-bipyridine ligand [48]. The essentially more planar coordination sphere in compound **12** bears resemblance to the published structures of **10** [38] and dichloro(2,2′-bipyridine)palladium(II) [49] with all the relevant bond lengths and angles well corresponding. The only inconsistent feature is the slight off-plane deviation of Cl1 and Cl21 (0.167(5) and 0.154(5) Å, respectively).

2.3. Nickel-catalyzed polymerization of ethylene

Each of the four dimeric catalyst precursor complexes (**6**–**9**) could be activated for ethylene polymerization by treatment with methylaluminoxane (MAO). Generally the catalytic behavior of these systems follows closely the trends observed previously for the related pyridinylimine complex [39]. In this study the variation in ligand structure, however, allows us to analyze, which features are due to reaction conditions and which result from the catalyst used. The polymerization conditions and results are summarized in Table 4.

Table 2
Selected bond lengths (Å) and angles (°) for complexes **6**–**9** *

6		**7**		**8**		**9**	
Bond lengths							
Ni–N1	2.069(5)	Ni1–N1	2.086(3)	Ni–N1	2.023(5)	Ni–N1	2.029(4)
		Ni2–N22	2.072(3)				
Ni–N8	2.042(5)	Ni1–N8	2.042(3)	Ni–N8	2.060(5)	Ni–N8	2.100(3)
		Ni2–N29	2.036(3)				
Ni–Br1	2.4759(17)	Ni1–Br1	2.5411(12)	Ni–Br1	2.5920(12)	Ni–Br1	2.5337(10)
		Ni2–Br3	2.5230(12)				
Ni–Br1a[a]	2.5479(12)	Ni1–Br1a[b]	2.4806(9)	Ni–Br1a[d]	2.4643(12)	Ni–Br1a[e]	2.4923(8)
		Ni2–Br3a[c]	2.4876(8)				
Ni–Br2	2.4139(18)	Ni1–Br2	2.4136(10)	Ni–Br2	2.4273(13)	Ni–Br2	2.4244(9)
		Ni2–Br4	2.4266(8)				
C6–C7	1.452(8)	C6–C7	1.469(6)	C6–C7	1.474(8)	C6–C7	1.490(6)
		C27–C28	1.454(6)				
C7–N8	1.265(8)	C7–N8	1.267(5)	C7–N8	1.280(7)	C7–N8	1.277(5)
		C28–N29	1.270(5)				
N8–C9	1.446(8)	N8–C9	1.461(5)	N8–C9	1.455(7)	N8–C9	1.455(5)
		N29–C30	1.460(5)				
Bond angles							
N1–Ni–N8	79.4(2)	N1–Ni1–N8	80.29(13)	N1–Ni–N8	79.61(19)	N1–Ni–N8	79.06(14)
		N22–Ni2–N29	80.55(13)				
N1–Ni–Br1	91.05(16)	N1–Ni1–Br1	175.99(9)	N1–Ni–Br1	84.02(14)	N1–Ni–Br1	91.51(10)
		N22–Ni2–Br3	176.09(10)				
N1–Ni–Br1a[a]	173.09(16)	N1–Ni1–Br1a[b]	91.58(10)	N1–Ni–Br1a[d]	169.29(14)	N1–Ni–Br1a[e]	166.67(11)
		N22–Ni2–Br3a[c]	90.74(10)				
N1–Ni–Br2	91.61(16)	N1–Ni1–Br2	92.17(9)	N1–Ni–Br2	92.66(13)	N1–Ni–Br2	92.01(11)
		N22–Ni2–Br4	90.97(10)				
N8–Ni–Br1	110.48(16)	N8–Ni1–Br1	99.32(10)	N8–Ni–Br1	114.91(12)	N8–Ni–Br1	145.74(10)
		N29–Ni2–Br3	99.75(10)				
N8–Ni–Br1a[a]	95.30(14)	N8–Ni1–Br1a[b]	107.95(10)	N8–Ni–Br1a[d]	103.25(13)	N8–Ni–Br1a[e]	96.37(10)
		N29–Ni2–Br3a[c]	106.33(9)				
N8–Ni–Br2	117.05(16)	N8–Ni1–Br2	108.95(10)	N8–Ni–Br2	108.57(12)	N8–Ni–Br2	104.25(10)
		N29–Ni2–Br4	107.94(9)				
Br1–Ni–Br1a[a]	86.63(4)	Br1–Ni1–Br1a[b]	84.73(3)	Br1–Ni–Br1a[d]	85.44(3)	Br1–Ni–Br1a[e]	85.30(3)
		Br3–Ni2–Br3a[c]	85.43(3)				
Br1–Ni–Br2	132.06(6)	Br1–Ni1–Br2	91.73(4)	Br1–Ni–Br2	134.89(4)	Br1–Ni–Br2	108.98(3)
		Br3–Ni2–Br4	92.64(2)				
Br1a[a]–Ni–Br2	94.78(4)	Br1a[b]–Ni1–Br2	143.02(3)	Br1a[d]–Ni–Br2	96.12(3)	Br1a[e]–Ni–Br2	101.27(3)
		Br3a[c]–Ni2–Br4	145.49(3)				
Ni–Br1–Nia[a]	93.37(4)	Ni1–Br1–Ni1a[b]	95.27(3)	Ni–Br1–Nia[d]	94.56(3)	Ni–Br1–Nia[e]	94.70(3)
		Ni2–Br3–Ni2a[c]	94.57(3)				

* Symmetry transformations used to generate equivalent atoms: [a] $-x, -y, -z+1$; [b] $-x+2, -y+1, -z+1$; [c] $-x+1, -y+1, -z$; [d] $-x+1, -y, -z+1$; [e] $-x+1, -y+1, -z+1$.

Table 3
Selected bond lengths (Å) and angles (°) for **10** [a], **11** and **12**

	10	**12**	**11**	
Bond lengths				
Pd–N1	2.028(3)	2.114(5)	Pd1–N1	2.025(4)
			Pd2–N21	2.026(4)
Pd–N8	2.022(3)	2.006(5)	Pd1–N8	2.021(4)
			Pd2–N28	2.023(4)
Pd–Cl1	2.2809(11)	2.2890(19)	Pd1–Cl1	2.2919(14)
			Pd2–Cl21	2.2897(15)
Pd–Cl2	2.2768(10)	2.260(2)	Pd1–Cl2	2.2703(16)
			Pd2–Cl22	2.2796(15)
C6–C7	1.457(5)	1.445(9)	C6–C7	1.445(6)
			C26–C27	1.447(6)
C7–N8	1.279(4)	1.286(9)	C7–N8	1.276(6)
			C27–N28	1.284(6)
N8–C9	1.448(4)	1.436(8)	N8–C9	1.444(6)
			N28–C29	1.438(5)
Bond angles				
N1–Pd–N8	80.08(11)	80.8(2)	N1–Pd1–N8	80.19(15)
			N21–Pd2–N28	80.38(15)
N1–Pd–Cl1	94.33(9)	101.98(16)	N1–Pd1–Cl1	94.92(11)
			N21–Pd2–Cl21	94.08(12)
N1–Pd–Cl2	174.51(9)	171.10(16)	N1–Pd1–Cl2	173.92(11)
			N21–Pd2–Cl22	174.29(11)
N8–Pd–Cl1	172.85(8)	172.66(15)	N8–Pd1–Cl1	174.53(11)
			N28–Pd2–Cl21	174.35(11)
N8–Pd–Cl2	94.64(8)	90.35(17)	N8–Pd1–Cl2	93.81(11)
			N28–Pd2–Cl22	93.93(11)
Cl1–Pd–Cl2	91.05(4)	86.90(7)	Cl1–Pd1–Cl2	91.12(6)
			Cl21–Pd2–Cl22	91.62(6)

[a] See Ref. [38].

All the catalysts lose activity with decreasing reaction temperature: the highest catalytic activities are obtained at 20°C (except for catalyst **9**/MAO) while lowering the temperature to 0°C leads to a significant decline in polymer production. Reduced polymer yields at 40°C (entries 1, 4, 7, and 10) can be attributed to catalyst decomposition [51], which is detected as diminishing ethylene consumption after initially higher activity. Nevertheless, activities for the system **7**/MAO, which contains a methyl substitute in the 6-position of the ligand pyridine ring, are one order of magnitude lower than for the unsubstituted complex [39]. This indicates severe interference from the protruding methyl group, which obstructs one of the equatorial coordination sites as can be seen in the solid-state structure as well (Fig. 2), thus, resulting in diminished activity. Also the phenyl group in the imino bridge of complex **9** has a slightly decreasing effect on the polymerization activity at higher temperatures (entries 11 and 12).

Although highly dependant on the polymerization temperature, the molecular weights of produced polymers are in general very similar, also with the values reported using the analogous catalyst [39], yet remain remarkably lower than obtained with the diazabutadiene systems under similar conditions [52]. Only a minor increase in chain length was achieved with the 6-methylpyridine-based catalyst **7**/MAO at 20 and 40°C (entries 4 and 5). Therefore, the dominating factor in controlling the molecular weight, besides reaction conditions, seems to be the steric bulk of the ligand, which is still lacking on the pyridine side despite the different modifications administered. As a result the blocking of the axial coordination sites in the nickel center, which according to theoretical calculations is essential in order to obtain higher molecular weights [17], remains insufficient and products with $M_w < 50\ 000$ g mol^{-1} are isolated.

The effect of ligand environment is most clear when polymer branching is analyzed. Even in this case polymerization temperature plays an important role, though the extent of branching can be controlled with the ligand structure. According to structural analysis by ^{13}C-NMR spectroscopy predominantly methyl-branched polymers are obtained. Decreasing the steric bulk in the aryl ring by replacing the two isopropyl groups with methyls in the 2- and 6-positions gives more linear polymers, as also theoretical [16] and experimental reports [14,53] on the diazabutadiene systems indicate, but quite remarkably the least branching was observed in samples produced with catalyst **7**/MAO, in which the isopropyl groups are present and the pyridine ring is substituted instead. Introduction of a methyl or phenyl side group to the imino carbon of the ligand, in turn, leads to increased branching, as happens with the diazabutadiene-based catalysts [14].

2.4. Palladium-catalyzed polymerization of norbornene

The palladium-based catalyst precursors **10**–**12** can be activated for norbornene polymerization by treatment with methylaluminoxane or by conversion into

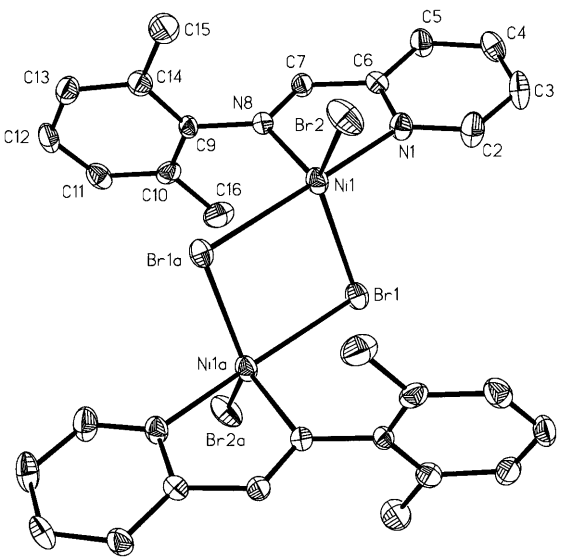

Fig. 1. Crystal structure of complex **6** with the labeling scheme. Displacement ellipsoids are drawn at the 40% probability level. Hydrogen atoms are omitted for clarity.

Table 4
Ethylene polymerization with catalysts **6**–**9**/MAO [a]

Entry	Catalyst	T_p (°C) [b]	n_{cat} (μmol) [c]	p (bar) [d]	Yield (g)	Activity [e]	M_w (g mol^{-1})	M_w/M_n	T_m (°C) [f]	Methyls per 1000 carbon atoms [g]
1	**6**	40	2.5	5.5	4.44	3600	2800	1.7	Wax	43
2	**6**	20	2.5	4.3	7.08	5700	5500	2.2	113.3 [h]	24
3	**6**	0	5.0	3.0	3.07	610	26 000	1.9	127.0	6
4	**7**	40	5.0	5.5	1.20	480	5600	2.2	116.7 [h]	28
5	**7**	20	10	4.3	2.93	590	7900	2.7	118.0 [h]	23
6	**7**	0	20	3.0	0.86	43	27 000	2.0	127.0	7
7	**8**	40	2.5	5.5	3.80	3000	3400	1.8	Wax	83
8	**8**	20	5.0	4.3	12.16	4800	5000	2.6	101.7 [h]	50
9	**8**	0	5.0	3.0	3.02	600	22 000	2.4	116.3	17
10	**9**	40	4.6	5.5	7.12	3100	2300	2.5	Wax	67
11	**9**	20	4.6	4.3	2.28	990	7000	2.1	101.3 [h]	53
12	**9**	0	4.6	3.0	4.64	1000	30 000	2.9	115.7	24

[a] [Al]:[M] = 2000, t_p = 30 min (except at 0°C 60 min).
[b] Polymerization temperature.
[c] Molar amount of the catalyst precursor (in μmol Ni).
[d] Ethylene pressure.
[e] Activity in kg PE (mol catalyst h)$^{-1}$.
[f] Peak melting temperature.
[g] Determined by ^{1}H-NMR spectroscopy.
[h] Broad melting peak.

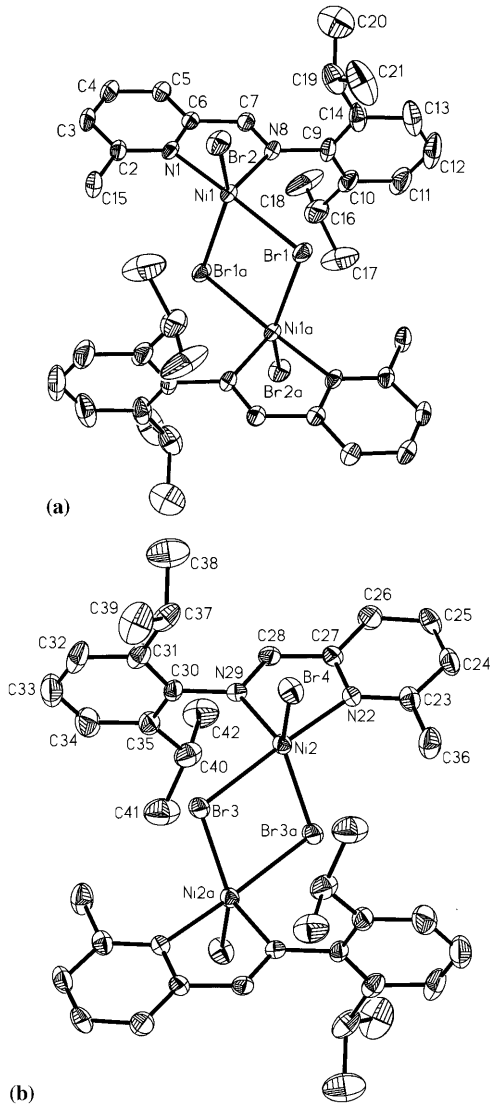

Fig. 2. Molecular structure of compound **7** showing the two crystallographically independent molecules of the asymmetric unit.

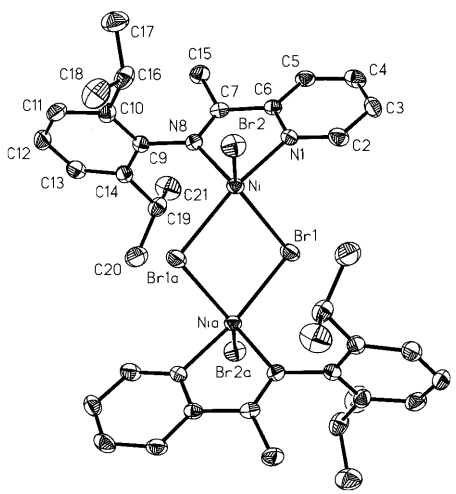

Fig. 3. Crystal structure of complex **8**.

the cationic species, except in the case of complex **11** for which only MAO-activation was possible, since the cationic compound was too unstable to be isolated. Altogether, the latter method seems to be more complicated requiring long reaction times and removal of the formed AgCl, which may disturb the polymerization [54], whereas MAO-activation can be performed in situ in a convenient manner. Polymerization results and conditions are summarized in Table 5.

Up to 100% monomer conversion was reached using MAO-containing catalyst systems (entries 5–10). In most cases the polymerization medium became highly

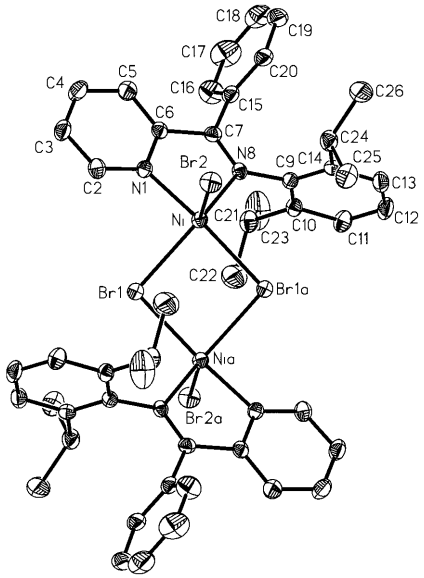

Fig. 4. Molecular structure of compound **9**. The solvent molecules are omitted for clarity.

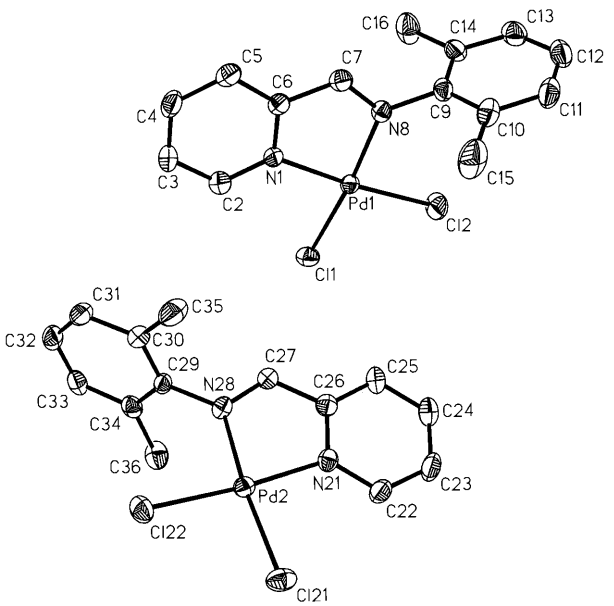

Fig. 5. Molecular structure of compound **11** showing the two crystallographically independent molecules of the asymmetric unit.

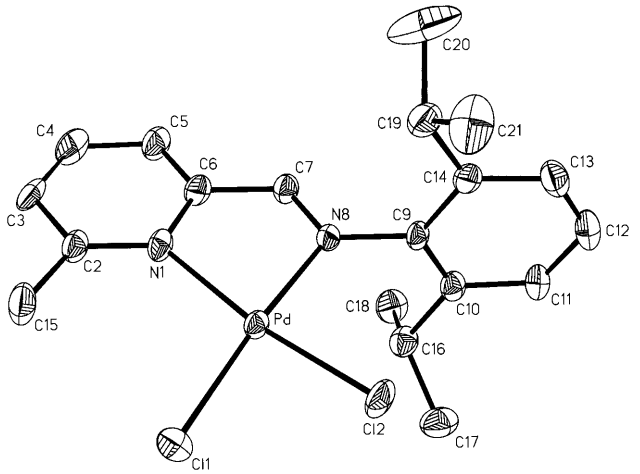

Fig. 6. Crystal structure of complex **12** with the labeling scheme.

viscous within the first 10 min of the 2 h polymerization run. Only catalyst **11**/MAO (entries 7 and 8) was unable to produce quantitative polymer yields in 2 h, which further demonstrates the inability of the dimethyl ligand (**2**) to sufficiently stabilize the cationic palladium center. Polymerizations with the single-component systems **13** and **14** (entries 1–4), in turn, showed disappointingly low yields ($<20\%$) compared to values reported for cationic diamine complexes (58–70%) [36] and traditional tetrakis(nitrile) systems (45–92%) [21,37] under similar conditions. Molecular weights of obtained polymers could not be determined by gel permeation chromatography due to insolubility of products in organic solvents, including 1,2,4-trichlorobenzene.

One possible explanation for the drastic difference in activity between the MAO-activated and single-component catalysts can be derived from the proposed polymerization mechanism [20,22] according to which the chain propagation step proceeds by insertion of the coordinated norbornene molecule into a metal–carbon bond (an analogous step is found in the mechanism of ethylene polymerization with transition metal catalysts [16]). The prerequisite palladium alkyl species [20] is readily generated in the reaction of methylaluminoxane and the catalyst precursor, thus promoting the insertion of the first monomer, while in the acetonitrile systems the initiation of polymerization seems to be less straightforward [55]. The significance of the direct palladium–carbon bond has been further demonstrated by the use of cationic palladium norbornyl derivatives as active catalysts [35]. Also the bulky size of the MAO counter ion, or the resulting weaker interaction with the metal center, may be beneficial to polymerization activity as in catalyst systems containing η^3-allyl ligands [32], although contrasting evidence has been described for the $[(RCN)_4Pd]^{2+}$ species [54].

3. Experimental

3.1. General

All complex preparations were performed under an argon atmosphere using standard Schlenk techniques. Acetone and acetonitrile were dried by storing under argon with $CaSO_4$ and $CaCl_2$ granules, respectively, other solvents by refluxing with a drying agent (CaH_2 for dichloromethane and sodium/benzophenone for the non-halogenated solvents) and distillation under argon. Commercial reagents, namely 6-methyl-2-pyridinecarboxaldehyde (Merck, 98%), 1-(2-pyridinyl)ethanone (Merck, 98%), phenyl-2-pyridinylmethanone (Merck, 98%), 2,6-di(1-methylethyl)phenylamine (Aldrich, 90%), bicyclo[2.2.1]hept-2-ene (Merck, 98%), methylaluminoxane (Witco, 30 wt.% solution in toluene) and silver tetrafluoroborate (Aldrich, 98%), were used as received. Dibromo(1,2-dimethoxyethane)nickel(II) [(DME)$NiBr_2$] [56], dichloro(1,5-cyclooctadiene)palladium(II) [(COD)$PdCl_2$] [57], 2,6-dimethyl-*N*-(2-pyridinylmethylene)-phenylamine (**2**) [44], 2,6-bis(1-methylethyl)-*N*-(2-

Table 5
Norbornene polymerization with catalysts **13**, **14** and **10**–**12**/MAO [a]

Entry	Catalyst	m_{cat} (mg) [b]	$n_{norbornene}:n_{cat}$ [c]	Yield (g)	Conversion (%)
1	**13**	50	400	0.18	6.0
2	**13**	50	800	0.21	3.5
3	**14**	50	400	0.55	19
4	**14**	50	800	Trace	–
5	**10**/MAO	25	400	2.16	100
6	**10**/MAO	25	800	4.22	100
7	**11**/MAO	25	400	2.29	94
8	**11**/MAO	25	800	4.74	98
9	**12**/MAO	25	400	2.10	100
10	**12**/MAO	25	800	4.11	100

[a] $T_p = 25$°C, $t_p = 120$ min; in entries 5–10 [Al]:[Pd] = 1000.
[b] Mass of the catalyst precursor.
[c] Monomer-to-catalyst ratio in mol:mol.

pyridinylmethylene)phenylamine (**1**) [38], and dichloro-[2,6-bis(1-methylethyl)-*N*-(2-pyridinylmethylene)phenylamine]palladium(II) (**10**) [38] were prepared as reported earlier. Synthesis products were characterized, when applicable, using a Varian Gemini 200 spectrometer (200 MHz) with $CDCl_3$ or acetone-d_6 as solvent and TMS as internal standard. Elemental analyses were carried out at the University of Ulm, Germany.

3.2. Ligand and complex preparation

3.2.1. 2,6-Bis(1-methylethyl)-N-[(6-methyl-2-pyridinyl)-methylene]phenylamine (3)

Ligand **3** was synthesized by modifying our recently reported method [38]. 6-Methyl-2-pyridinecarboxaldehyde (9.70 g, 80.1 mmol) was dissolved in 100 ml of ethanol and 2,6-di(1-methylethyl)phenylamine (15.80 g, 80.2 mmol) was added. This mixture was refluxed for 30 min and after solvent evaporation subjected to column chromatography on basic alumina with pentane–ethyl acetate (3:1) as eluent. Recrystallization from a 1:3 mixture of ethanol and pentane at −18°C afforded pale yellow, needle-like crystals. Yield: 11.84 g (53%). Anal. Calc. for $C_{19}H_{24}N_2$ (280.41): C, 81.38; H, 8.63; N, 9.99. Found: C, 81.05; H, 8.56; N, 9.95%. ^{1}H-NMR ($CDCl_3$): δ 1.09 (d, 12 H, H_{Me}), 2.57 (s, 3 H, $H_{pyridine,6\text{-}Me}$), 2.89 (m, 2 H, C*H*Me$_2$), 7.04–7.13 (m, 3 H, H_{phenyl}), 7.20 (d, 1 H, $H_{pyridine,5}$), 7.66 (t, 1 H, $H_{pyridine,4}$), 8.02 (d, 1 H, $H_{pyridine,3}$), 8.20 (s, 1 H, C*H*=N) ppm.

3.2.2. 2,6-Bis(1-methylethyl)-N-[1-(2-pyridinyl)-ethylidene]phenylamine (4)

The ketone 1-(2-pyridinyl)ethanone (1.82 g, 15.0 mmol) was combined with 2,6-di(1-methylethyl)-phenylamine (3.57 g, 18.1 mmol) and three drops of concentrated H_2SO_4 as well as some sodium sulfate was added. This mixture was heated to 120°C and stirring was continued at this temperature for 24 h. The dark brown, oily raw product was dissolved in 50 ml of dichloromethane, filtered, washed with 50 ml of water and dried with Na_2SO_4. After filtration and solvent evaporation the yellow–brown residue was purified by crystallization from ethanol affording yellow, cubic crystals. Yield: 1.41 g (34%). Anal. Calc. for $C_{19}H_{24}N_2$ (280.41): C, 81.38; H, 8.63; N, 9.99. Found: C, 81.36; H, 8.65; N, 10.21%. ^{1}H-NMR ($CDCl_3$): δ 1.15 (d, 12 H, H_{Me}), 2.21 (s, 3 H, $H_{bridge\text{-}Me}$), 2.75 (m, 2 H, C*H*Me$_2$), 7.11–7.20 (m, 3 H, H_{phenyl}), 7.39 (m, 1 H, $H_{pyridine,5}$), 7.82 (t, 1 H, $H_{pyridine,4}$), 8.36 (d, 1 H, $H_{pyridine,3}$), 8.69 (d, 1 H, $H_{pyridine,6}$) ppm.

3.2.3. 2,6-Bis(1-methylethyl)-N-(phenyl-2-pyridinylmethylene)phenylamine (5)

Analogously to the preparation of **4**, compound **5** was synthesized from phenyl-2-pyridinylmethanone (2.75 g, 15.0 mmol) and 2,6-di(1-methylethyl)-phenylamine (3.29 g, 16.7 mmol) at 120°C. The ligand was obtained from ethanol as bright yellow microcrystalline powder. Yield: 1.68 g (33%). Anal. Calc. for $C_{24}H_{26}N_2$ (342.48): C, 84.17; H, 7.65; N, 8.18. Found: C, 84.04; H, 7.72; N, 8.37%. ^{1}H-NMR ($CDCl_3$): δ 0.90 (d, 3 H, H_{Me}), 0.97 (d, 3 H, H_{Me}), 1.14 (d, 6 H, H_{Me}), 2.93 (m, 2 H, C*H*Me$_2$), 6.98–7.23 (m, 6 H, H_{arom}), 7.45 (m, H_{arom}), 7.83 (m, H_{arom}), 8.25 (d, H_{arom}), 8.64 (m, H_{arom}) ppm.

3.2.4. Di-μ-bromodibromobis[2,6-dimethyl-N-(2-pyridinylmethylene)phenylamine]dinickel(II) (6)

To a suspension of [(DME)$NiBr_2$] (2.03 g, 6.6 mmol) in 20 ml of CH_2Cl_2 was added the solution of ligand **2** (1.42 g, 6.8 mmol) in 20 ml of CH_2Cl_2. The orange–red reaction mixture was stirred for 24 h at room temperature (r.t.), after which the precipitate was collected by filtration, washed with pentane (2 × 10 ml), and vacuum-dried yielding complex **6** as an orange–yellow powder. Yield: 1.55 g (55%). Anal. Calc. for $C_{28}H_{28}Br_4N_4Ni_2$ (857.55): C, 39.22; H, 3.29; N, 6.53. Found: C, 38.97; H, 3.60; N, 6.39%.

Compounds **7**–**9** were prepared analogously from [(DME)$NiBr_2$] and the corresponding ligand in dichloromethane.

3.2.5. Di-μ-bromodibromobis{2,6-bis(1-methylethyl)-N-[(6-methyl-2-pyridinyl)methylene]phenylamine}-dinickel(II) (7)

Orange–yellow powder. Yield: 57%. Anal. Calc. for $C_{38}H_{28}Br_4N_4Ni_2$ (997.82): C, 45.74; H, 4.85; N, 5.61. Found: C, 45.56; H, 4.81; N, 5.53%.

3.2.6. Di-μ-bromodibromobis{2,6-bis(1-methylethyl)-N-[1-(2-pyridinyl)ethylidene]phenylamine}dinickel(II) (8)

Bright orange powder. Yield: 62%. Anal. Calc. for $C_{38}H_{28}Br_4N_4Ni_2$ (997.82): C, 45.74; H, 4.85; N, 5.61. Found: C, 45.44; H, 4.84; N, 5.69%.

3.2.7. Di-μ-bromodibromobis[2,6-bis(1-methylethyl)-N-(phenyl-2-pyridinylmethylene)phenylamine]dinickel(II) (9)

Orange–brown powder. Yield: 77%. Anal. Calc. for $C_{48}H_{52}Br_4N_4Ni_2{\cdot}CH_2Cl_2$ (1206.89): C, 48.76; H, 4.51; N, 4.64. Found: C, 48.44; H, 5.05; N, 4.55%.

3.2.8. Dichloro[2,6-dimethyl-N-(2-pyridinylmethylene)-phenylamine]palladium(II) (11)

A solution of [(COD)$PdCl_2$] (0.50 g, 1.8 mmol) in 30 ml of CH_2Cl_2 was combined with a solution of ligand **2** (0.39 g, 1.9 mmol) in 10 ml of CH_2Cl_2. The resulting orange–yellow solution was stirred at ambient temperature for 24 h at which time a precipitate was observed. The pale orange powder was recovered by filtration, washed with diethyl ether (2 × 20 ml), filtered and

vacuum dried. Yield: 0.52 g (75%). Anal. Calc. for $C_{14}H_{14}Cl_2N_2Pd$ (387.60): C, 43.38; H, 3.64; N, 7.23. Found: C, 43.38; H, 3.68; N, 7.21%. ^{1}H-NMR (acetone-d_6): δ 2.21 (s, 6 H, H_{Me}), 6.94–7.06 (m, 3 H, H_{phenyl}), 7.90 (m, 1 H, $H_{pyridine,5}$), 8.16 (d, 1 H, $H_{pyridine,3}$), 8.34 (t, 1 H, $H_{pyridine,4}$), 8.57 (s, 1 H, C*H*=N), 9.16 (d, 1 H, $H_{pyridine,6}$) ppm.

3.2.9. Dichloro{2,6-bis(1-methylethyl)-N-[(6-methyl-2-pyridinyl)methylene]phenylamine}palladium(II) (12)

The analogous complex **12** was prepared from [(COD)PdCl$_2$] (0.80 g, 2.8 mmol) and **3** (0.81 g, 2.9 mmol) following the method described above. Yield: 0.76 g (60%). Anal. Calc. for $C_{19}H_{24}Cl_2N_2Pd$ (457.73): C, 49.86; H, 5.28; N, 6.12. Found: C, 49.92; H, 5.30; N, 6.07%. ^{1}H-NMR (acetone-d_6): δ 1.01 (d, 6 H, H_{Me}), 1.24 (d, 6 H, H_{Me}), 3.01 (s, 3 H, $H_{pyridine,6\text{-}Me}$), 3.29 (m, 2 H, C*H*Me$_2$), 7.05–7.19 (m, 3 H, H_{phenyl}), 7.70 (d, 1 H, $H_{pyridine,5}$), 8.02 (d, 1 H, $H_{pyridine,3}$), 8.16 (t, 1 H, $H_{pyridine,4}$), 8.59 (s, 1 H, C*H*=N) ppm.

3.2.10. Bis(acetonitrile)[2,6-bis(1-methylethyl)-N-(2-pyridinylmethylene)phenylamine]palladium(II)-bis(tetrafluoroborate) (13)

The neutral dichloropalladium compound **10** (0.22 g, 0.49 mmol in 50 ml of CH_3CN) was converted to the corresponding cationic complex by reacting with $AgBF_4$ (0.19 g, 0.99 mmol) for 96 h at r.t. The reaction mixture was filtered to remove the precipitated AgCl and evaporated to dryness leaving a yellow residue, which was then dissolved in CH_2Cl_2. After filtration, solvent evaporation and drying under vacuum complex **13** was obtained as pale yellow powder. Yield: 0.28 g (89%). ^{1}H-NMR (acetone-d_6): δ 1.10 (d, 6 H, H_{Me}), 1.35 (d, 6 H, H_{Me}), 1.91 (s, 6 H, H_{MeCN}), 3.63 (m, 2 H, C*H*Me$_2$), 7.26–7.47 (m, 3 H, H_{phenyl}), 7.95 (m, 1 H, $H_{pyridine,5}$), 8.43 (d, 1 H, $H_{pyridine,3}$), 8.54 (t, 1 H, $H_{pyridine,4}$), 8.84 (s, 1 H, C*H*=N), 8.96 (d, 1 H, $H_{pyridine,6}$) ppm.

3.2.11. Bis(acetonitrile){2,6-bis(1-methylethyl)-N-[(6-methyl-2-pyridinyl)methylene]phenylamine}-palladium(II)bis(tetrafluoroborate) (14)

Analogously to the preparation of **13**, complex **14** was synthesized from compound **12** (0.40 g, 0.87 mmol) and $AgBF_4$ (0.34 g, 1.7 mmol) in 50 ml of acetonitrile and collected as pale yellow powder. Yield: 0.41 g (73%). ^{1}H-NMR (acetone-d_6): δ 1.09 (d, 6 H, H_{Me}), 1.35 (d, 6 H, H_{Me}), 1.91 (s, 6 H, H_{MeCN}), 2.61 (s, 3 H, $H_{pyridine,6\text{-}Me}$), 3.58 (m, 2 H, C*H*Me$_2$), 7.24–7.49 (m, 3 H, H_{phenyl}), 7.83 (d, 1 H, $H_{pyridine,5}$), 8.23 (d, 1 H, $H_{pyridine,3}$), 8.33 (t, 1 H, $H_{pyridine,4}$), 8.72 (s, 1 H, C*H*=N) ppm.

3.3. X-ray crystallography

The crystals were mounted to a glass fiber using the oil drop method [58]. Crystal data obtained with the ω–2θ scan mode were collected on an automated four-circle Rigaku AFC-7S diffractometer using graphite-monochromatized Mo–K$_\alpha$ radiation (λ = 0.71073 Å) at 193 K (except for complex **8** at 213 K). Three standard reflections were monitored after every 200 intensity scans. The intensities were corrected for Lorentz and polarization effects. For all compounds ψ-scans were used for absorption correction [59]. Data sets were compressed to reflection files with TEXSAN single crystal structure analysis software [60]. Structure solution using direct methods and further refinement with full-matrix least-squares on F^2 was carried out with SHELX-97 [61]. All non-hydrogen atoms were refined anisotropically. Hydrogen atoms were introduced to calculated positions (riding model) with 1.2 times the displacement factors of the host carbon atoms (see Section 4).

3.4. Polymerization experiments

Ethylene polymerization runs were performed at constant monomer concentration. The polymerization procedure and equipment have been described in detail previously [39]. For polymer molecular weights and molecular weight distributions a Waters 150-C GPC chromatograph was used operating at 135°C with 1,2,4-trichlorobenzene solvent and polystyrene calibration standards. Melting temperatures of preheated and cooled samples were determined by differential scanning calorimetry using a Perkin–Elmer DSC-2 calorimeter. Analysis of polymer microstructure was based on NMR spectra recorded on a Varian XL-300 spectrometer at 125°C. Samples were dissolved in 1,1,2,2-tetrachloroethane-d_2 and a 10:1 weight ratio mixture of 1,2,4-trichlorobenzene and benzene-d_6 for ^{1}H- and ^{13}C-NMR measurements, respectively.

For the polymerization of norbornene the palladium catalyst was dissolved in the polymerization medium consisting of dichloromethane (50 ml), 1,2-dichlorobenzene (5 ml), and nitrobenzene (1 ml) in a 250-ml Schlenk flask. When MAO-activation was used (Table 5, entries 5–10) the reaction was performed in toluene (80 ml). Polymerization was commenced by adding the appropriate amount of norbornene monomer (and MAO cocatalyst, in entries 5–10). After stirring for 2 h at ambient temperature the reaction was quenched by addition of methanol acidified with a small amount of aqueous HCl. The precipitated polymer was collected by filtration, washed with methanol and dried under vacuum.

4. Supplementary material

Crystallographic data for the structural analysis have been deposited with the Cambridge Crystallographic Data Centre, CCDC-133658 (for **6**), 133659 (for **7**), 133660 (for **8**), 133661 (for **9**), 127783 (for **11**), and 127782 (for **12**). Copies of this information can be obtained free of charge from: The Director, CCDC, 12 Union Road, Cambridge, CB2 1EZ, UK (fax: +44-1223-336-033; e-mail: deposit@ccdc.cam.ac.uk or www: http://www.ccdc.cam.ac.uk).

Acknowledgements

Financial support from the Academy of Finland and the Technology Development Center of Finland (TEKES) is gratefully acknowledged. The authors wish to thank Alexandra Abele (University of Ulm, Germany) and Kimmo Hakala (Helsinki University of Technology, Finland) for providing the EA and polymer NMR measurements, respectively.

References

[1] A.A. Montagna, R.M. Burkhart, A.H. Dekmezian, Chemtech 27 (1997) 26.
[2] A.M. Thayer, Chem. Eng. News 73 (1995) 15.
[3] H.H. Brintzinger, D. Fischer, R. Mülhaupt, B. Rieger, R.M. Waymouth, Angew. Chem. Int. Ed. Engl. 34 (1995) 1143.
[4] W. Kaminsky, Macromol. Chem. Phys. 197 (1996) 3907.
[5] M. Bochmann, J. Chem. Soc. Dalton Trans. (1996) 255.
[6] W. Kaminsky, M. Arndt, Adv. Polym. Sci. 127 (1997) 143.
[7] G.J.P. Britovsek, V.C. Gibson, D.F. Wass, Angew. Chem. Int. Ed. Engl. 38 (1999) 429.
[8] V.C. Gibson, P.J. Maddox, C. Newton, C. Redshaw, G.A. Solan, A.J.P. White, D.J. Williams, Chem. Commun. (1998) 1651.
[9] B.L. Small, M. Brookhart, A.M.A. Bennett, J. Am. Chem. Soc. 120 (1998) 4049.
[10] G.J.P. Britovsek, V.C. Gibson, B.S. Kimberley, P.J. Maddox, S.J. McTavish, G.S. Solan, A.J.P. White, D.J. Williams, Chem. Commun. (1998) 849.
[11] A.M. al-Jarallah, J.A. Anabtawi, M.A.B. Siddiqui, A.M. Aitani, A.W. al-Sa'doun, Catal. Today 14 (1992) 42.
[12] W. Keim, A. Behr, M. Röper, in: G. Wilkinson, F.G.A. Stone, E.W. Abel (Eds.), Comprehensive Organometallic Chemistry, vol. 8, Pergamon, Oxford, 1982 (Chapter 56.2).
[13] P.W. Jolly, in: G. Wilkinson, F.G.A. Stone, E.W. Abel (Eds.), Comprehensive Organometallic Chemistry, vol. 8, Pergamon, Oxford, 1982 (Chapter 52.2).
[14] L.K. Johnson, C.M. Killian, M. Brookhart, J. Am. Chem. Soc. 117 (1995) 6414.
[15] L.K. Johnson, C.M. Killian, S.D. Arthur, J. Feldman, E.F. McCord, S.J. McLain, K.A. Kreutzer, M.A. Bennett, E.B. Coughlin, S.D. Ittel, A. Parthasarathy, D.J. Tempel, M.S. Brookhart, PCT Int. Appl. 96/23010 (1996).
[16] D.G. Musaev, R.D.J. Froese, K. Morokuma, New J. Chem. 21 (1997) 1269.
[17] L. Deng, T.K. Woo, L. Cavallo, P.M. Margl, T. Ziegler, J. Am. Chem. Soc. 119 (1997) 6177.
[18] C.M. Killian, L.K. Johnson, M. Brookhart, Organometallics 16 (1997) 2005.
[19] S.A. Svejda, M. Brookhart, Organometallics 18 (1999) 65.
[20] N. Seehof, C. Mehler, S. Breunig, W. Risse, J. Mol. Catal. 76 (1992) 219.
[21] T.F.A. Haselwander, W. Heitz, S.A. Krügel, J.H. Wendorff, Macromol. Chem. Phys. 197 (1996) 3435.
[22] C. Mehler, W. Risse, Makromol. Chem. Rapid Commun. 12 (1991) 255.
[23] U. Peucker, W. Heitz, Macromol. Rapid Commun. 19 (1998) 159.
[24] B.L. Goodall, L.H. McIntosh III, L.F. Rhodes, Macromol. Symp. 89 (1995) 421.
[25] J.E. McKeon, P.S. Starcher, US Pat. 3,330,815 (1967).
[26] C. Taniélian, A. Kiennemann, T. Osparpucu, Can. J. Chem. 57 (1979) 2022.
[27] A. Sen, T.-W. Lai, R.R. Thomas, J. Organomet. Chem. 358 (1988) 567.
[28] J. Melia, S. Rush, J.P. Mathew, E. Connor, C. Mehler, S. Breunig, W. Risse, Polym. Prepr. (Am. Chem. Soc. Div. Polym. Chem.) 35 (1994) 518.
[29] J.P. Mathew, A. Reinmuth, J. Melia, N. Swords, W. Risse, Macromolecules 29 (1996) 2755.
[30] J. Melia, E. Connor, S. Rush, S. Breunig, C. Mehler, W. Risse, Macromol. Symp. 89 (1995) 433.
[31] C. Mehler, W. Risse, Macromolecules 25 (1992) 4226.
[32] A. Reinmuth, J.P. Mathew, J. Melia, W. Risse, Macromol. Rapid Commun. 17 (1996) 173.
[33] B.S. Heinz, W. Heitz, S.A. Krügel, F. Raubacher, J.H. Wendorff, Acta Polym. 48 (1997) 385.
[34] B.L. Goodall, L.H. McIntosh, PCT Int. Appl. 98/56839 (1998).
[35] B.S. Heinz, F.P. Alt, W. Heitz, Macromol. Rapid Commun. 19 (1998) 251.
[36] A.S. Abu-Surrah, B. Rieger, J. Mol. Catal. A: Chem. 128 (1998) 239.
[37] M. Arndt, M. Gosmann, Polym. Bull. 41 (1998) 433.
[38] T.V. Laine, M. Klinga, M. Leskelä, Eur. J. Inorg. Chem. (1999) 959.
[39] T.V. Laine, K. Lappalainen, J. Liimatta, E. Aitola, B. Löfgren, M. Leskelä, Macromol. Rapid Commun. 20 (1999) 487.
[40] L.K. Johnson, J. Feldman, K.A. Kreutzer, S.J. McLain, A.M.A. Bennett, E.B. Coughlin, D.S. Donald, L.T.J. Nelson, A. Parthasarathy, X. Shen, W. Tam, Y. Wang, PCT Int. Appl. 97/02298 (1997).
[41] P.-L. Bres, V.C. Gibson, C.D.F. Mabille, W. Reed, D. Wass, R.H. Weatherhead, PCT Int. Appl. 98/49208 (1998).
[42] M. Geprägs, G. Luinstra, P. Brinkmann, PCT Int. Appl. 99/03867 (1999).
[43] S.P. Meneghetti, P.J. Lutz, J. Kress, Organometallics 18 (1999) 2734.
[44] G. Schmauss, P. Barth, Z. Naturforsch. Teil B 25 (1970) 789.
[45] L. Strekowski, M.T. Cegla, D.B. Harden, S.-B. Kong, J. Org. Chem. 54 (1989) 2464.
[46] B.E. Love, J. Ren, J. Org. Chem. 58 (1993) 5556.
[47] R.E. Rülke, J.G.P. Delis, A.M. Groot, C.J. Elsevier, P.W.N.M. van Leeuwen, K. Vrieze, K. Goubitz, H. Schenk, J. Organomet. Chem. 508 (1996) 109.
[48] G.R. Newkome, F.R. Fronczek, V.K. Gupta, W.E. Puckett, D.C. Pantaleo, G.E. Kiefer, J. Am. Chem. Soc. 104 (1982) 1782.
[49] M. Maekawa, M. Munakata, S. Kitagawa, M. Nakamura, Anal. Sci. 7 (1991) 521.
[50] P.D. Beer, N.C. Fletcher, M.G.B. Drew, T.J. Wear, Polyhedron 16 (1997) 815.
[51] R.F. de Souza, R.S. Mauler, L.C. Simon, F.F. Nunes, D.V.S. Vescia, A. Cavagnolli, Macromol. Rapid Commun. 18 (1997) 795.

[52] T.V. Laine, M. Klinga, A. Maaninen, E. Aitola, M. Leskelä, Acta Chem. Scand. 53 (1999) 968.
[53] D. Pappalardo, M. Mazzeo, C. Pellecchia, Macromol. Rapid Commun. 18 (1997) 1017.
[54] T.F.A. Haselwander, W. Heitz, M. Maskos, Macromol. Rapid Commun. 18 (1997) 689.
[55] J. Feldman, S.J. McLain, A. Parthasarathy, W.J. Marshall, J.C. Calabrese, S.D. Arthur, Organometallics 16 (1997) 1514.
[56] L.G.L. Ward, Inorg. Synth. 12 (1972) 154.
[57] D. Drew, J.R. Doyle, Inorg. Synth. 13 (1972) 47.
[58] T. Kottke, D. Stalke, J. Appl. Crystallogr. 26 (1993) 615.
[59] A.C.T. North, D.C. Phillips, F.S. Mathews, Acta Crystallogr. Sect. A 24 (1968) 351.
[60] TEXSAN: Single Crystal Structure Analysis Software, Version 1.6, Molecular Structure Corporation, The Woodlands, TX, 1993.
[61] G.M. Sheldrick, SHELX-97, Program for the Solution and Refinement of Crystal Structures, University of Göttingen, Germany, 1997.